Electronic, magnetic, and structural properties of $CrMnSb_{0.5}Si_{0.5}$

Lukas Stuelke,[1] Lilit Margaryan,[2] Parashu Kharel,[3] Paul M. Shand,[1] and Pavel V. Lukashev[1,#]

[1]*Department of Physics, University of Northern Iowa, Cedar Falls, IA 50614, USA*
[2]*College and Science and Engineering, American University of Armenia, Yerevan 0019, Republic of Armenia*
[3]*Department of Physics, South Dakota State University, Brookings, SD 57007, USA*

E-mail: pavel.lukashev@uni.edu

Abstract

Half-metallic Heusler compounds are among the most actively studied materials for applications in spin-based devices. Largely, this is due to their higher Curie temperature compared with the other half-metallic compounds, and relative ease of fabrication. Here we theoretically study one such Heusler alloy $CrMnSb_{0.5}Si_{0.5}$. In particular, we demonstrate a potential stability of this compound by estimating its formation energy, its half-metallic electronic structure (stable under a considered range of biaxial strain), and ferrimagnetic alignment. The calculated Curie temperature of this material is 787 K, much higher than room temperature. At the same time, we have shown that in thin-film geometry the spin-polarization of this material is strongly reduced due to the emergence of surface states in the minority-spin energy gap. In addition, one of the considered termination surfaces is thermodynamically unstable, while the other is stable. The presented results may be useful for researchers working on practical applications in the field of spintronics.

I. Introduction

For practical device applications in the field of spin-based electronics (spintronics), one needs materials with large spin-polarization and high Curie temperature. In recent years, Heusler alloys have been actively studied for such applications, as they may provide ideal spin-polarization of 100% (half-metallicity), and Curie temperatures much higher than room temperature.[1,2,3,4,5,6,7,8] In addition, some of these materials have been reported to exhibit compensated ferrimagnetic alignment, which is a very attractive feature for applications where stray magnetic fields are to be avoided.[9,10,11,12,13,14] In addition to full Heusler and half Heusler compounds, quaternary Heusler

alloys attracted a lot of attention recently, as they allow additional flexibility for controlling the electronic and magnetic properties by tuning the stoichiometry.[15,16,17]

Some of the Heusler alloys exhibit what may be called "quasi half-metallic" electronic structure, where the spin-polarization is less than 100%, but a half-metallic transition may be induced by some external stimuli, such as mechanical strain. Typically, in these materials the Fermi level is located fairly close to the energy gap of one of the spin channels, and the half-metallic transition is induced by its rigid shift into the gap.[18] This mechanism may serve as an example of combining what has been recently labeled as "straintronics"[19,20] with spintronics. At the same time, reaching large values of mechanical strain even in thin-film geometry is not always practically feasible. One possible alternative is to mimic the actual mechanical strain with atomic substitution. For example, if an element with a larger atomic radius is replaced with an element with a smaller atomic radius, this may result in reduced volume of the unit cell, i.e. effectively in a compressive strain.

In our recent work we predicted that a half-metallic electronic structure along with fully compensated ferrimagnetic alignment may be induced by chemical substitution of Sb with P in CrMnSb, i.e. in $CrMnSb_{0.5}P_{0.5}$.[21] More specifically, the substitution of Sb with P results in reduction of the equilibrium lattice parameter, which shifts the Fermi level into the minority-spin energy gap. The substitution with phosphorus, however, may be undesirable for practical applications, due to its high flammability. Therefore, one may consider substituting Sb with another non-magnetic element, with an atomic radius smaller than that of Sb. Here, we demonstrate that replacing P with Si also leads to half-metallic electronic structure, although without fully compensated ferrimagnetic alignment, i.e. the net magnetic moment is not zero. In addition, our calculations indicate that in thin-film geometry the minority-spin energy gap is populated with surface states, strongly reducing the spin polarization.

The rest of the paper is organized as follows. In Section II, we briefly outline the computational methods and techniques. Sections III contains our main results and consists of three parts: the first part covers the bulk properties of $CrMnSb_{0.5}Si_{0.5}$, the second part describes how these properties are affected by reduced geometry, and the third part discusses energetic stability of this compound. Sections IV contains concluding remarks, and is followed by acknowledgments and references.

II. Computational Methods

All calculations in this work are performed with the Vienna *ab initio* simulation package (VASP),[22] within the projector augmented-wave method (PAW)[23] and generalized-gradient approximation (GGA) scheme proposed by Perdew, Burke, and Ernzerhof.[24] The cut-off energy of the plane-waves is set to 500 eV, and we used the integration method by Methfessel and Paxton with a 0.05 eV width of smearing.[25] The total energy and electronic structure calculations are performed with the energy convergence criteria of 10^{-3} meV. The Brillouin-zone integration is performed with a *k*-point mesh of 12 × 12 × 12 for bulk, and 12 × 12 × 1 for thin-film calculations. For biaxial strain calculations, we fixed the in-plane lattice parameters, and optimized the out-of-plane coordinates, with the energy convergence criteria of 10^{-2} meV. Some of the results and figures are obtained using the MedeA® software environment.[26] All calculations are performed using Extreme Science and Engineering Discovery Environment (XSEDE) resources located at the Pittsburgh Supercomputing Center (PSC)[27], and at a local computer cluster located at the University of Northern Iowa (UNI).

III. Results and Discussion

III-1. Bulk

CrMnSb belongs to a class of half-Heusler compounds, which may crystallize in the so called α- and γ- phases. For detailed description of these phases, see e.g. Ref. [28]. For CrMnSb, the γ- phase is energetically favorable,[21] and therefore we focus on this structure in the rest of the paper. In our recent work, we showed that in its ground state, CrMnSb is "nearly" half-metallic, however a half-metallic transition may be induced by a compressive strain.[21] Such compression may be difficult to achieve mechanically, but it may be induced by chemical substitution of Sb with a smaller non-magnetic atom. Fig. 1 (a) shows the crystal structure of $CrMnSb_{0.5}Si_{0.5}$, where half of the Sb atoms in the parent compound CrMnSb have been replaced with Si. Fig. 1 (b) shows calculated density of states (DOS) of this alloy, which clearly exhibits a half-metallic profile, with a minority-spin energy gap of around 0.8 eV. The calculated equilibrium lattice constant is $a = 5.706$ Å, as indicated in the figure.

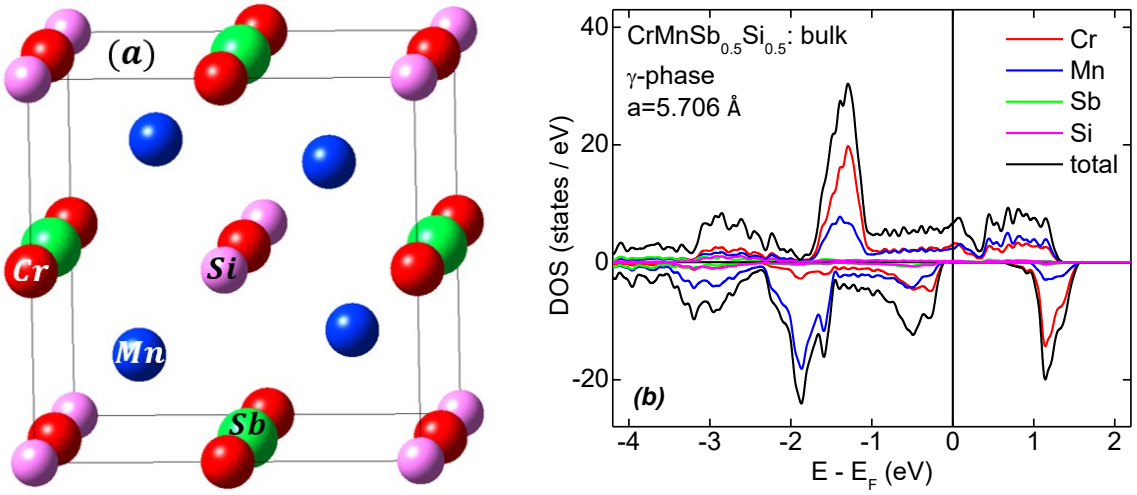

Figure 1: Crystal structure of $CrMnSb_{0.5}Si_{0.5}$ in the γ-phase. Atoms are color-coded as indicated in the figure: Cr – red, Mn – blue, Sb – green, Si – magenta; (b) Calculated density of states of bulk $CrMnSb_{0.5}Si_{0.5}$ in the γ-phase. Atomic contributions are color-coded as indicated in the figure.

In spin-based electronics applications, such as in magnetic tunnel junctions (MTJ), materials are often arranged in multilayer thin-film geometry.[29] In such arrangement, effect of mechanical strain and reduced geometry should be taken into account. We address these two questions in the rest of this section and in the next sub-sections.

Fig. 2 shows calculated total density of states of $CrMnSb_{0.5}Si_{0.5}$ under uniform pressure (a) and biaxial strain (b), for various lattice constants (indicated in the figure). For biaxial strain calculations, the in-plane lattice parameters were fixed at the values shown in Fig. 2 (b), while the out-of-plane lattice constants were optimized. The calculated $c\ vs.\ a$ data (out-of-plane vs. in-plane lattice parameter) for these calculations are shown in Fig. 4 (c).

As shown in Fig. 2 (a), application of uniform expansion shifts the Fermi level towards the minority-spin valence states, and at $a \approx 5.750$ Å (around 0.8% expansion) it crosses the highest occupied spin-down state. At the same time, a uniform compression / expansion is not a realistic mechanism in thin-film applications, where one should instead consider the effect of biaxial strain. As shown in Fig. 2 (b), tensile strain also eventually destroys half-metallicity, but in a less dramatic way. In particular, the Fermi level crosses the highest occupied minority-spin state at $a \approx 5.800$ Å, corresponding to around 1.6% increase of the in-plane lattice parameter. This indicates that

$CrMnSb_{0.5}Si_{0.5}$ may retain its perfect spin polarization in practical settings, except at relatively large values of tensile strain.

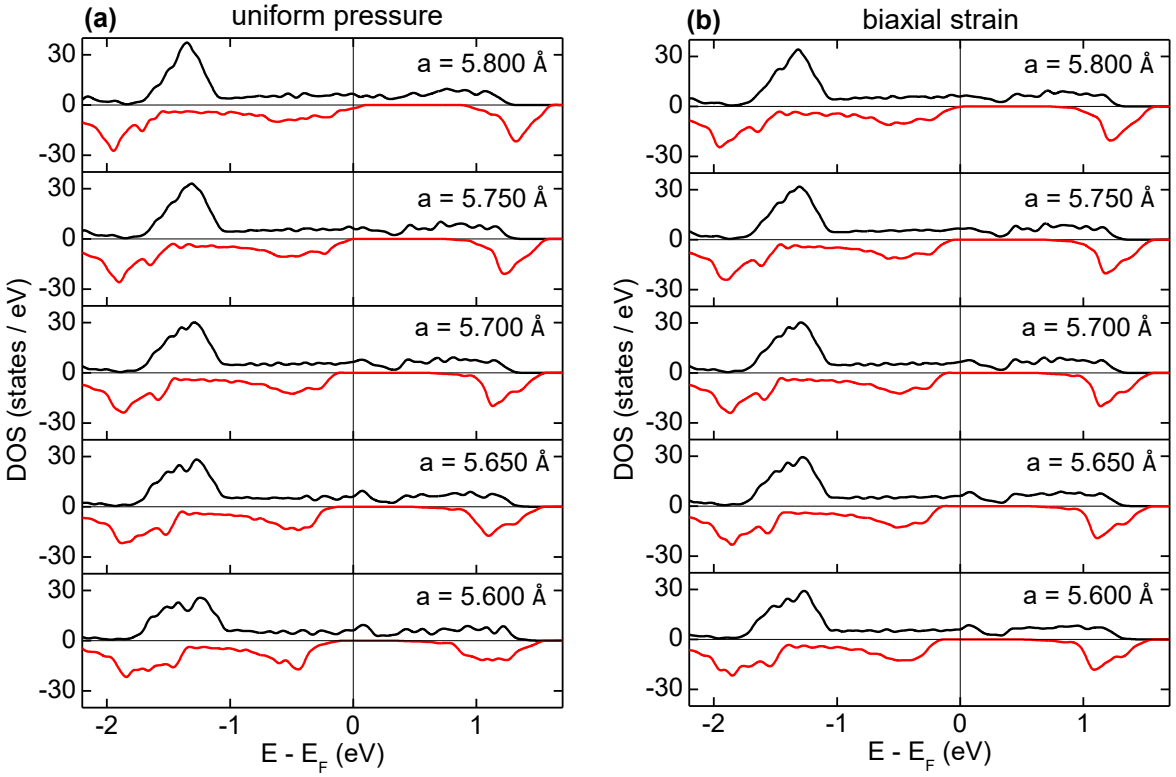

Figure 2: Calculated density of states of bulk $CrMnSb_{0.5}Si_{0.5}$ in the γ-phase as a function of lattice constant, for uniform compression / expansion (a) and for biaxial strain (b). Positive and negative DOS correspond to majority- and minority- spin states, respectively. In-plane lattice parameters at which DOS is calculated are indicated in the figure.

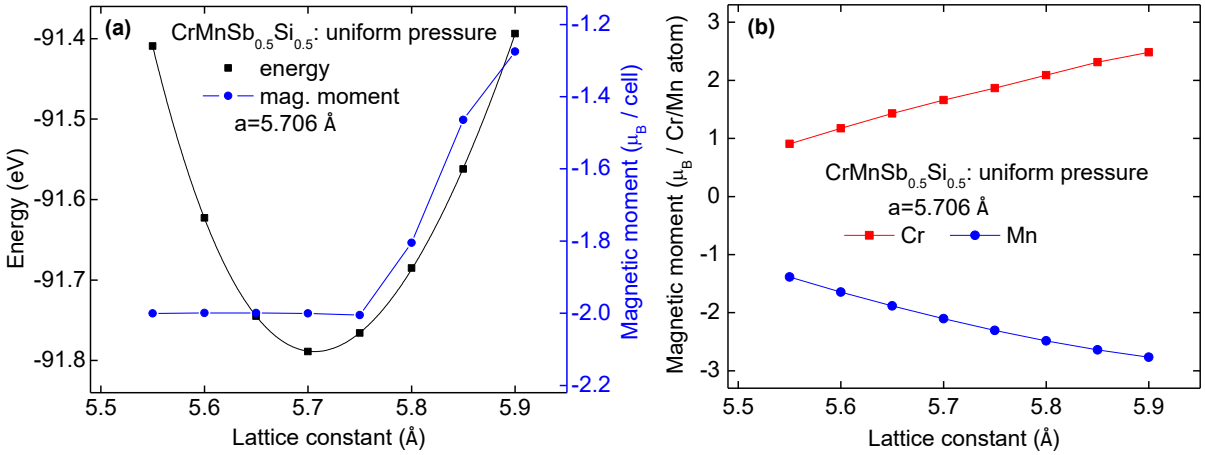

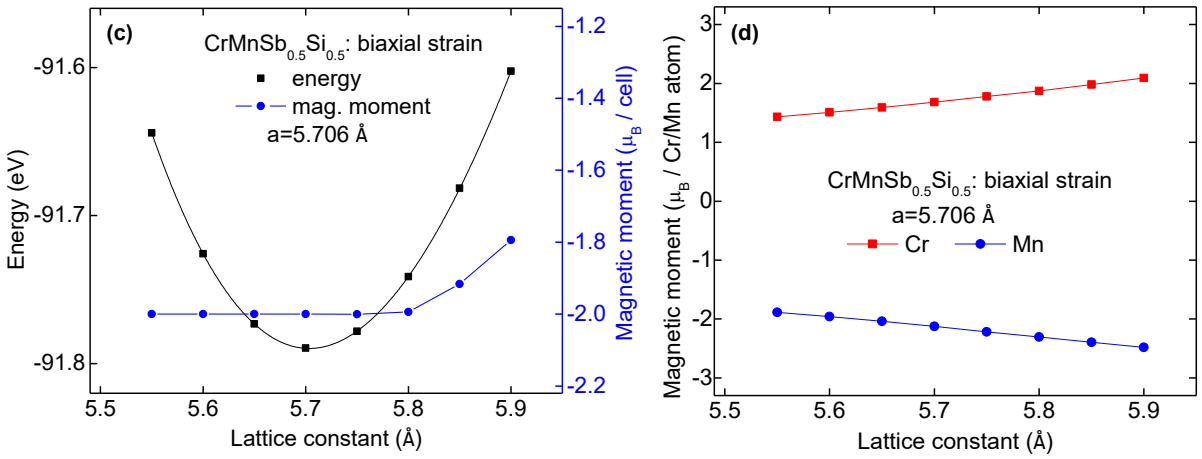

Figure 3: Calculated energy (black line and squares) and total magnetic moment per 12-atom cell (blue line and circles) of bulk $CrMnSb_{0.5}Si_{0.5}$ in the γ-phase as a function of lattice constant, for uniform compression / expansion (a) and biaxial strain (c). Calculated magnetic moments per Cr atom (red line and squares) and Mn atom (blue line and circles) of bulk $CrMnSb_{0.5}Si_{0.5}$ in the γ-phase as a function of lattice constant, for uniform compression/expansion (c) and biaxial strain (d).

Next, we turn our attention to the magnetic structure of $CrMnSb_{0.5}Si_{0.5}$ in the ground state and under uniform pressure / biaxial strain. Figure 3 summarizes our results. In particular, Fig. 3 (a) shows calculated total energy (black line and squares) and total magnetic moment (blue line and circles) per 12-atom cell of $CrMnSb_{0.5}Si_{0.5}$ under uniform pressure. Figure 3 (b) shows calculated magnetic moments per Cr (red line and squares) and Mn (blue line and circles) atoms under uniform pressure (magnetic moments of Sb and Si are negligible and not included / discussed in this work). Figures 3 (c) and (d) are corresponding plots calculated under biaxial strain.

The main two results shown in Fig. 3 are the ferrimagnetic alignment of Cr and Mn atoms, and integer total magnetic moment of 2 μ_B per 12-atom cell in the range of pressure / strain corresponding to the half-metallic electronic structure. The integral total magnetic moment serves as another confirmation of 100% spin polarization, since in this case the Fermi level is located in the energy gap of the minority-spin channel, which results in all valence band states of that channel being occupied. As a result, the total number of these states is an integer, leading to an integral total magnetic moment (the total valence charge is an integer). The deviation from the integral total magnetic moment takes place at $a \approx 5.750$ Å for uniform pressure, and at $a \approx 5.800$ Å for biaxial strain, consistent with the results reported above (see Fig. 2).

We also estimated the Curie temperature of $CrMnSb_{0.5}Si_{0.5}$ within the mean field approximation framework, as follows: $T_c = \frac{2||E_{FiM}|-|E_{FM}||}{3nk_B}$.[30,31] Here, n is the number of magnetic atoms in the cell (8, in our case), and $E_{FiM} = -91.789473\ eV$ and $E_{FM} = -90.977200\ eV$ are calculated energies of ferrimagnetic and ferromagnetic arrangements, correspondingly. The calculated value of T_c is 787 K, i.e. much higher than room temperature. In addition, the calculated values of E_{FiM} and E_{FM} confirm the stability of the ferrimagnetic phase.

III-2. Thin film

A perfect spin polarization of half-metallic compounds is often detrimentally affected in thin film geometry due to the emergence of surface states in the energy gap.[32,33,34] In fact, a thin film half-metallicity is rather uncommon, although in certain cases a 100% spin polarization in Heusler alloys may be preserved, depending on the surface termination.[35,36] To address this question, we calculated the electronic structure of $CrMnSb_{0.5}Si_{0.5}$ in thin film geometry, as illustrated in Fig. 4 (a). Here, four 12-atom cells of $CrMnSb_{0.5}Si_{0.5}$ are stacked together in (001) direction, with a 20 Å layer added to avoid a potential overlap of the surface wave functions due to the imposed periodic boundary condition. The in-plane lattice constant is fixed at the bulk value of 5.706 Å, while the out-of-plane atomic positions are fully relaxed.

Fig. 4 (b) shows calculated cell-resolved density of states, with the numbering of the cells consistent with the one shown in Fig. 4 (a). The electronic structure of cell 2 (black line) is half-metallic, closely resembling the bulk-like features, which indicates that the thickness of the considered cell is adequate to describe the thin film properties of the material. At the same time, both Mn and $CrSb_{0.5}Si_{0.5}$ terminations result in reduced spin polarization due to the emergence of surface states in the minority-spin band gap. The reduction of spin polarization is very strong. In particular, the spin polarization of cell 1 is 34% (blue line), while the spin polarization of cell 3 is only around 9% (red line). These values are calculated from the data shown in Fig. 4 (a), using the following expression: $P = \big(N_{\uparrow}(E_F) - N_{\downarrow}(E_F)\big)/\big(N_{\uparrow}(E_F) + N_{\downarrow}(E_F)\big)$, where P is the spin polarization, while $N_{\uparrow\downarrow}(E_F)$ is the spin-dependent density of states at the Fermi level, E_F.[37]

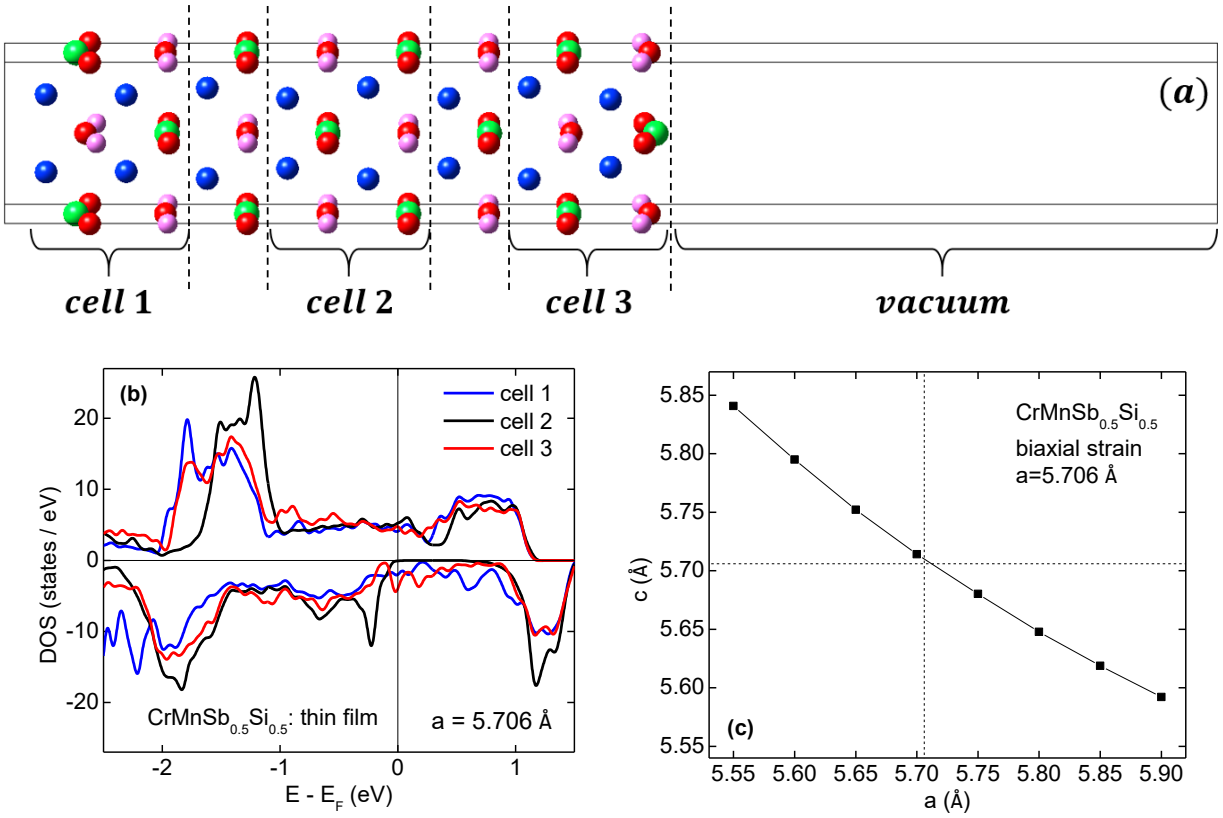

Figure 4: (a) Crystal structure of thin-film $CrMnSb_{0.5}Si_{0.5}$ in the γ-phase after atomic relaxation: atoms are color coded similar to Fig. 1, i.e. Cr – red, Mn – blue, Sb – green, Si – magenta; (b) Calculated cell-resolved density of states of thin-film $CrMnSb_{0.5}Si_{0.5}$ in the γ-phase, with numbering of the cells consistent with the one shown in Fig. 2 (a); (c) Calculate out-of-plane vs. in-plane lattice constant (c vs. a) of bulk $CrMnSb_{0.5}Si_{0.5}$ in the γ-phase under biaxial strain.

Fig. 5 shows calculated cell- *and element*- resolved density of states of thin film $CrMnSb_{0.5}Si_{0.5}$, with the numbering of the cells consistent with the one shown in Fig. 4 (a). For comparison, bulk DOS is also shown. As one can see from Fig. 5 (b) and (d), the bulk and cell 2 electronic structures are very similar, which confirms again that the thickness of the cell used in our thin film calculations is adequate for simulating this system. At the same time, as illustrated in Fig. 5 (a) and (c), the main contribution to the minority-spin surface states comes from Cr and Mn, while a sizeable contribution from Si is also visible at $CrSb_{0.5}Si_{0.5}$ – terminated cell. This probably indicates that other possible terminations, not considered in the current work, will likely also exhibit reduced spin polarization due to the emergence of the minority-spin surface states.

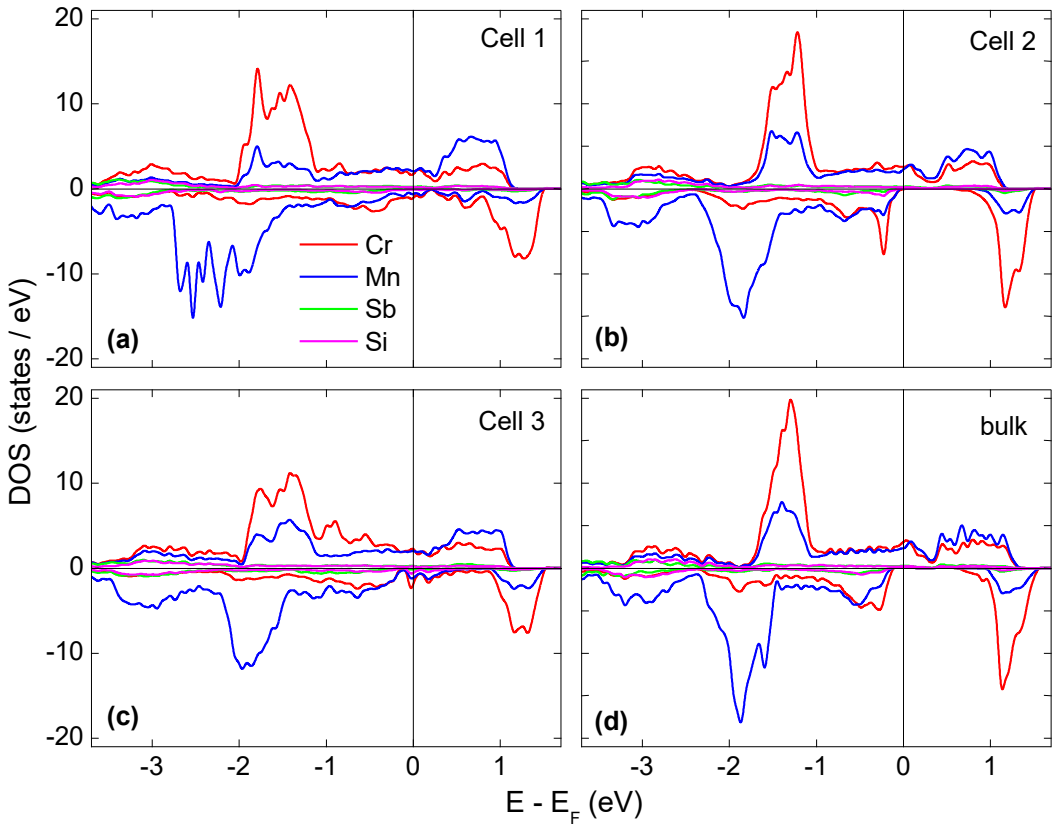

Figure 5: Calculated element- and cell- resolved DOS of thin-film $CrMnSb_{0.5}Si_{0.5}$ ((a) – cell 1, (b) – cell 2, (c) – cell 3), with numbering of the cells consistent with the one shown in Fig. 2 (a), and elemental contributions colored as indicate in the figure. For comparison, bulk DOS (d) is also shown.

	Cell 1	Cell 2	Cell 3	Bulk
m / Cr (μ_B)	2.153	1.730	2.383	1.686
m / Mn (μ_B)	- 2.678	- 2.153	-1.953	-2.130
m / f.u. (μ_B)	-0.525	-0.423	0.430	-0.444

Table 1. Calculated magnetic moments in thin film $CrMnSb_{0.5}Si_{0.5}$. The last column shows the corresponding bulk values.

The magnetic structure of the considered thin film cell is ferrimagnetic, similar to the bulk magnetic alignment. Table 1 shows the calculated atom resolved and cell resolved magnetic moments in the thin film cell. The last column includes the bulk values, for comparison. It should

be emphasized that the sum of atomic moments is slightly different from the total magnetic moment because the local magnetization and charge are estimated in atomic spheres, which do not fill the entire space of the unit cell precisely.[8]

Next, we estimate the relative stability of the two considered termination surfaces, Mn and $CrSb_{0.5}Si_{0.5}$. In particular, we calculate their surface free energies, as follows.

$$E_{surface,Mn} = \frac{1}{2}(E_{Mn-term} - N_{Cr} \times E_{Cr} - N_{Mn} \times E_{Mn} - N_{Sb} \times E_{Sb} - N_{Si} \times E_{Si})/a \quad (1)$$

$$E_{surface,CrSb_{0.5}Si_{0.5}} = \frac{1}{2}\left(E_{CrSb_{0.5}Si_{0.5}} - N_{Cr} \times E_{Cr} - N_{Mn} \times E_{Mn} - N_{Sb} \times E_{Sb} - N_{Si} \times E_{Si}\right)/a \quad (2)$$

Here, $E_{surface,Mn}$ / $E_{surface,CrSb_{0.5}Si_{0.5}}$ are surface energies of Mn – / $CrSb_{0.5}Si_{0.5}$ – terminated cells, $E_{Mn-term}$ / $E_{CrSb_{0.5}Si_{0.5}}$ are calculated total energies of Mn – / $CrSb_{0.5}Si_{0.5}$ – terminated cells, E_{Cr}, E_{Mn}, E_{Mn}, E_{Si} are calculated energies per atom of Cr, Mn, Sb, and Si in bulk geometry, N_{Cr}, N_{Mn}, N_{Sb}, N_{Si} are the numbers of Cr, Mn, Sb, and Si atoms in the corresponding thin-film cell, a is the in-plane surface area of the thin-film cell. For estimating $E_{Mn-term}$ and $E_{CrSb_{0.5}Si_{0.5}}$, we performed additional calculations for symmetrically terminated $CrMnSb_{0.5}Si_{0.5}$ thin film. More specifically, in the thin film cell shown in Fig. 4 (a), we removed the leftmost atomic monolayer to simulate the $CrSb_{0.5}Si_{0.5}$ – terminated cell, and the rightmost monolayer to simulate the Mn – terminated cell. Then we fully relaxed the atomic positions, while the in-plane lattice constant was fixed at the bulk value of $a = 5.706$ Å. The calculated surface energies are $E_{surface,Mn} = 0.0013 \frac{eV}{Å^2}$; $E_{surface,CrSb_{0.5}Si_{0.5}} = -0.0423 \frac{eV}{Å^2}$. These values indicate that the Mn – terminated cell is thermodynamically unstable, while the $CrSb_{0.5}Si_{0.5}$ – terminated cell is stable, and may be potentially realized experimentally. At the same time, as was shown above, the spin-polarization of the $CrSb_{0.5}Si_{0.5}$ – terminated cell is only 9%. Thus, if this material is synthesized in thin film geometry, it is likely that its spin-polarization will be strongly reduced due to the presence of the minority-spin surface states.

A strong reduction of the spin polarization due to the emergence of minority-spin surface states may limit the potential applicability of $CrMnSb_{0.5}Si_{0.5}$ for spintronic devices. Yet, it should be noted that in principle the half-metallicity of certain Heusler alloys, such as NiMnSb could be also restored, by interface engineering in thin film geometry.[38,39]

III-3. Energetic stability

To the best of our knowledge, the alloy discussed in this work has not yet been synthesized experimentally. To check the potential stability of $CrMnSb_{0.5}Si_{0.5}$, we have estimated its formation energy, as follows.

$$E_{form}(Cr_4Mn_4Sb_2Si_2) = E(Cr_4Mn_4Sb_2Si_2) - 4 \times \big(E(Cr) + E(Mn)\big) - 2 \times \big(E(Sb) + E(Si)\big)$$

Here, $E_{form}(Cr_4Mn_4Sb_2Si_2)$ is the formation energy, $E(Cr_4Mn_4Sb_2Si_2)$ is the energy per corresponding cell, while $E(Cr), E(Mn), E(Sb)$ and $E(Si)$ are energies per corresponding atom. The numerical subscripts indicate the number of atoms in the cell.

The calculated formation energy is

$$E_{form}(Cr_4Mn_4Sb_2Si_2) = E(Cr_4Mn_4Sb_2Si_2) - 4 \times \big(E(Cr) + E(Mn)\big) - 2 \times \big(E(Sb) + E(Si)\big) =$$

$$-91.78947306 - 4 \times (-9.49218318 - 8.72109886) - 2 \times (-3.72784391 - 5.00001932) \rightarrow$$

$$E_{form}(Cr_4Mn_4Sb_2Si_2) = -1.48061844\ eV$$

The negative value of $E_{form}(Cr_4Mn_4Sb_2Si_2)$ indicates a potential stability of this alloy. In addition, we also confirmed that a phase separation of $Cr_4Mn_4Sb_2Si_2$ into $Cr_4Mn_4Sb_4$ and $Cr_4Mn_4Si_4$ is unlikely by comparing the energy of $E(Cr_4Mn_4Sb_2Si_2)$ with the energies $E(Cr_4Mn_4Sb_4)$ and $E(Cr_4Mn_4Si_4)$, all three calculated at $a = 5.706$ Å, i.e. the equilibrium lattice constant of $Cr_4Mn_4Sb_2Si_2$. The results are shown in the expression below, with the negative value of the final answer confirming a potential stability of $CrMnSb_{0.5}Si_{0.5}$.

$$E(Cr_4Mn_4Sb_2Si_2) - \frac{1}{2}\big(E(Cr_4Mn_4Sb_4) + E(Cr_4Mn_4Si_4)\big) =$$

$$= -91.78947306 - \frac{1}{2}(-88.47692593 - 94.85632389) = -0.12284815\ eV$$

IV. Conclusions

In conclusion, using first principles calculations we showed that a half-Heusler compound $CrMnSb_{0.5}Si_{0.5}$ is a half-metallic ferrimagnet (magnetic moments of Cr and Mn are anti-aligned) in the ground state, and it retains its half-metallic electronic structure under a considerable range of mechanical strain. The estimated Curie temperature of this material is 787 K, much higher than

room temperature. At the same time, in thin-film geometry the spin-polarization of this alloy is strongly reduced due to the emergence of minority-spin surface states in the energy gap. The energetic stability of $CrMnSb_{0.5}Si_{0.5}$ is confirmed by estimating its formation energy, and the energy required for the phase separation into $Cr_4Mn_4Sb_4$ and $Cr_4Mn_4Si_4$. The results reported in this work may be useful for researchers working on practical applications in the field of spin-based electronics.

Acknowledgments

This research is supported by the National Science Foundation (NSF) under Grant Numbers 2003828 and 2003856 via DMR and EPSCoR. This work used the Extreme Science and Engineering Discovery Environment (XSEDE), which is supported by National Science Foundation grant number ACI-1548562. This work used the XSEDE Regular Memory (Bridges 2) and Storage (Bridges Ocean) at the Pittsburgh Supercomputing Center (PSC) through allocation TG-DMR180059, and the resources of the Center for Functional Nanomaterials, which is a U.S. DOE Office of Science Facility, and the Scientific Data and Computing Center, a component of the Computational Science Initiative, at Brookhaven National Laboratory (BNL) under Contract No. DE-SC0012704. P.L. thanks Wesley Jones from the IT Department of UNI for his help with a local computer cluster.

Data availability statement

The data that support the findings of this study are available upon reasonable request from the authors.

References

[1] R. A. de Groot, F. M. Mueller, P. G. van Engen, and K. H. J. Buschow, Phys. Rev. Lett. **50**, 2024 (1983).
[2] I. Galanakis, P. H. Dederichs, N. Papanikolaou, Phys. Rev. B **66**, 174429 (2002).
[3] E. Şaşıoğlu, L. M. Sandratskii, and P. Bruno, Phys. Rev. B **72**, 184415, (2005).
[4] B. Balke, G. H. Fecher, J. Winterlik, and C. Felser, Appl. Phys. Lett. **90**, 152504 (2007).

[5] H. Kurt, K. Rode, M. Venkatesan, P. Stamenov, and J. M. D. Coey, Phys. Status Solidi B **248**, 2338 (2011).
[6] J. Winterlik, S. Chadov, A. Gupta, V. Alijani, T. Gasi, K. Filsinger, B. Balke, G. H. Fecher, C. A. Jenkins, F. Casper, J. Kübler, G. Liu, L. Gao, S. S. P. Parkin, and C. Felser, Adv. Mater. **24**, 6283 (2012).
[7] I. Galanakis, in *Heusler Alloys*, Springer Series in Materials Science 222, C. Felser and A. Hirohata (eds.), Springer International Publishing Switzerland 2016.
[8] P. Lukashev, P. Kharel, S. Gilbert, B. Staten, N. Hurley, R. Fuglsby, Y. Huh, S. Valloppilly, W. Zhang, K. Yang, R. Skomski, and D. J. Sellmyer, Appl. Phys. Lett. **108**, 141901 (2016).
[9] H. van Leuken and R. A. de Groot, Phys. Rev. Lett. **74**, 1171 (1995).
[10] E. Şaşıoğlu, Phys. Rev. B **79**, 100406(R) (2009).
[11] I. Galanakis, and E. Şaşıoğlu, Appl. Phys. Lett. **99**, 052509 (2011).
[12] A. Bouabça, H. Rozale, A. Amar, Wang X.T., A. Sayade, A. Lakdja, Chinese Journal of Physics, **54**, 489 (2016).
[13] R. Stinshoff, A. K. Nayak, G. H. Fecher, B. Balke, S. Ouardi, Y. Skourski, T. Nakamura, and C. Felser, Phys. Rev. B **95**, 060410(R) (2017).
[14] J. Han, X. Wu, Y. Feng and G. Gao, J. Phys.: Condens. Matter **31**, 305501 (2019).
[15] S. Berri, J. Magn. Magn. Mater. **401**, 667 (2016).
[16] S. Berri, J. Supercond. Nov. Magn. **29**, 1309 (2016).
[17] S. Berri, Chin. J. Phys. **55**, 195 (2017).
[18] I. Tutic, et al., J. Phys.: Condens. Matter **29**, 075801 (2017).
[19] A. Bukharaev, A. Zvezdin, A. Pyatakov, and Y. Fetisov, Phys.-Usp. **61**, 1175 (2018).
[20] F. Miao, S. Liang, and Bin Cheng, npj Quantum Materials **6**, 59 (2021).
[21] E. O'Leary, et al., J. Appl. Phys., **128**, 113906 (2020).
[22] G. Kresse and D. Joubert, Phys. Rev. B **59**, 1758 (1999).
[23] P. Blöchl, Phys. Rev. B **50**, 17953 (1994).
[24] J. P. Perdew, K. Burke, and M. Ernzerhof, Phys. Rev. Lett. **77**, 3865 (1996).
[25] M. Methfessel and A. T. Paxton, Phys. Rev. B **40**, 3616 (1989).
[26] MedeA-2.22, Materials Design, Inc., San Diego, CA, USA, 2017.
[27] J. Towns, T. Cockerill, M. Dahan, I. Foster, K. Gaither, A. Grimshaw, V. Hazlewood, S. Lathrop, D. Lifka, G. D. Peterson, R. Roskies, J. R. Scott, N. Wilkins-Diehr, "XSEDE: Accelerating Scientific Discovery", Computing in Science & Engineering, vol.**16**, no. 5, pp. 62-74, Sept.-Oct. 2014.
[28] M. Shaughnessy, L. Damewood, C. Y. Fong, L. H. Yang, and C. Felser, J. of App. Phys. **113**, 043709 (2013).
[29] E. Tsymbal, O. Mryasov, and P. LeClair, J. Phys.: Condens. Matter **15**, R109 (2003).
[30] E. Sasioglu, L. M. Sandratskii, P. Bruno, J. Phys.: Condens. Matter **17**, 995 (2005).
[31] M. Rostami, M. Afkani, M. Torkamani, F. Kanjouri, Mater. Chem. Phys. **248**,122923 (2020).
[32] I. Galanakis, J. Phys.: Condens. Matter **14**, 6329 (2002).
[33] W. Zhu, B. Sinkovic, E. Vescovo, C. Tanaka, and J. S. Moodera, Phys. Rev. B **64**, 060403(R) (2001).
[34] A. N. Caruso, C. N. Borca, D. Ristoiu, J. P. Nozières, P. A. Dowben, Surf. Sci. **525**, L109 (2003).
[35] J. Herran, R. Carlile, P. Kharel, and P. V. Lukashev, J. Phys.: Condens. Matter **31**, 495801 (2019).
[36] S. Prophet, R. Dalal, P. R. Kharel, and P. V Lukashev, J. Phys.: Condens. Matter **31**, 055801 (2019).
[37] J. P. Velev, P. A. Dowben, E. Y. Tsymbal, S. J. Jenkins, and A. N. Caruso, Surf. Sci. Rep. **63**, 400 (2008).
[38] G.A. Wijs, R.A. de Groot, Phys. Rev. B **64**, R020402 (2001).
[39] A. Debernardi, M. Peressi, A. Baldereschi, Mater. Sci. Eng. C-Bio. S **23**, 743 (2003).